Solvent-Dependent Photophysical Properties of a Phenothiazone Dye as an Optical Probe

Soichi Otsuki* and Takahisa Taguchi

Osaka National Research Institute, AIST, 1-8-31 Midorigaoka, Ikeda, Osaka 563

(Received April 22, 1996)

A phenothiazone dye, 7-dimethylamino-3*H*-phenothiazin-3-one, was investigated as an optical probe in homogeneous media. Two absorption bands appeared in aprotic solvents and dioxane–water and exhibited different dependencies on the solvent polarity/polarizability scale, π^*. Both of the bands were quite different from that corresponding to the aggregated molecules or the protonated species of the dye. These results suggest the existence of two ground-state species with non-twisted and twisted conformations of the 7-amino group. The π^* dependencies of the fluorescence maxima and the rate constants of the fluorescence decays showed three types of behavior in dioxane–water. The Lippert–Mataga plot of the spectral shift was interpreted by assuming two types of behavior in aprotic solvents. These facts suggest that the fluorescence comes from three emitting states which exist in fast equilibria. The strong polarity dependencies and the long wavelengths of the absorption and fluorescence, the large Stokes shift, and the appreciable fluorescence quantum yield make the dye useful as an optical probe of the polarity of a variety of microenvironments.

Fluorimetry using extrinsic molecular probes has been used to determine the polarity and viscosity of the microenvironment of biological and synthetic molecular systems. A number of fluorescent probes have since been developed, including *N*-arylaminonaphthalenesulfonates[1,2] and 6-acyl-2-dimethylaminonaphthalenes.[3] However, most probes are limited by their ultraviolet or near ultraviolet excitation maxima. Long wavelengths of excitation and emission in fluorimetry may be expected to offer several advantages such as minimized interference from chromophores of target molecules or from other probes, a reduction of radiation damage to the target molecules, decreased scattering of light, and so on.[4,5] In order to realize useful excitation and emission properties, the development and characterization of fluorescence probes is required.

A phenothiazone dye, 7-dimethylamino-3*H*-phenothiazin-3-one (DMPT), which is known by the common name of Methylen Violet (Bernthsen), has both electron-donating and electron-withdrawing groups attached to the conjugated aromatic system. In such a molecule, the first singlet state offers an internal charge transfer character and a much larger dipole moment than the ground state. Consequently, a high sensitivity of the fluorescence to the polarity and a large Stokes shift are expected. In addition, it seems that the presence of two hetero atoms in the aromatic ring shifts the absorption and fluorescence to the red.

Thus, DMPT is a bright prospect as an optical probe working at long wavelengths, although no previous work has been done on its photophysical properties except for second-order nonlinear optical behavior studies.[6] In this paper, a detailed examination of the solvent dependence of the photophysical properties of DMPT is reported. These results provide valuable information for the utilization of this probe in studies on the microenvironments of various media.

Experimental

Materials. Benzene, toluene, dioxane, ethyl acetate, and acetone were of reagent-grade quality and were distilled before use. Spectroscopy-grade acetonitrile, pyridine, dimethylformamide (DMF), and dimethyl sulfoxide (DMSO) (Katayama) were used as received. Water was deionized and distilled. *N*, *N*-dimethyl-3-nitroaniline (98%; Aldrich) was purified by recrystallization. Laser-grade Rhodamine 6G (Exiton) was used as received. *N*, *N*-dimethyl-4-nitroaniline (Ishidzu) and 4-nitroanisole (Katayama) were of reagent-grade quality and were used as received. DMPT (87%; Aldrich) was purified by recrystallization from 1,2-dichloroethane.

Apparatus and Methods. Absorption spectra were recorded on a Shimadzu UV-2200 spectrophotometer. Fluorescence emission and excitation spectra were recorded on a Hitachi F-3010 spectrofluorimeter with excitation and emission slits of 5 nm. The emission spectra were measured by exciting samples at 530 nm and were corrected using *N*, *N*-dimethyl-3-nitroaniline in benzene–hexane as a standard. The excitation spectra were obtained by calibrating the excitation system using an optically dense solution of Rhodamine B in ethylene glycol. Fluorescence quantum yields were determined using Rhodamine 6G in ethanol ($\phi_f = 0.95$) as a standard. Fluorescence lifetimes were measured on a Horiba NAES-1100 photon-counting apparatus equipped with a Toshiba KL-51 or KL-53 bandpass filter on the excitation side and a monochrometer with a slit width of 14 nm on the emission side. The wavelength of the monochrometer was set at the maximum of the steady-state fluorescence spectrum.

Unless otherwise stated, the experiments were performed with freshly prepared dilute solutions ($2—2.5\times10^{-6}$ M, 1 M = 1 mol dm^{-3}). The solutions were not degassed.

Solvatochromic scales introduced by Taft and Kamlet[7] were used for analyzing the absorption and fluorescence properties of DMPT. Scales for pure solvents were taken from the literature.[8,9]

Scales for dioxane–water were experimentally determined. The polarity/polarizability π^* was determined from the absorption maxima of *N*, *N*-dimethyl-4-nitroaniline (**1**) according to the following equation.[9]

$$\pi^* = 8.006 - 0.2841\nu_{max}\ (\mathbf{1}) \quad (1)$$

In this equation and all those following, ν_{max} values are in units of 10^3 cm^{-1}. The hydrogen-bond acidity α was determined from the absorption maxima of 4-nitroanisole (**2**) and Reichardt's betaine, 2, 6-diphenyl-4-(2,4,6-triphenylpyridinio)phenolate (**3**) according to the following equation.[9]

$$\alpha = [\nu_{max}\ (\mathbf{3}) + 1.873\nu_{max}\ (\mathbf{2}) - 74.58]/6.24 \quad (2)$$

The ν_{max} (**1**) and ν_{max} (**2**) values were measured in our laboratory, although the ν_{max} (**3**) value was taken or derived by interpolation from values in the literature.[10]

Results

Optical Absorption Behaviors. Figure 1 shows the absorption spectra of DMPT in various aprotic solvents. The absorption band undergoes a significant red shift when increasing the polarity of the solvent, which is accompanied by a change in the spectral shape. A single band in nonpolar solvents such as benzene changes to one having a long-wavelength shoulder in polar solvents such as DMSO.

Figure 2 shows the absorption spectra of DMPT in dioxane–water. The spectral change is parallel to that appearing in the aprotic solvents but is much more significant. A single band peaking at 532 nm in pure dioxane shifts to a longer wavelength with decreasing dioxane content (band I). A new band (band II) appears at the long-wavelength side of band I below a dioxane content of 90 wt%. As the dioxane content decreases to 50 wt%, band I reduces and band II develops. These results suggest that two different chemical species of DMPT exist in dioxane–water and that their ratios change with solvent composition.

Shifts of absorption spectra of organic dyes can be analyzed in relation to solvatochromic scales as introduced by Taft and Kamlet. For a variety of dyes, a plot of the absorption maximum vs. the polarity/polarizability parameter π^* gives a straight line in non-hydrogen-bonding solvents whereas in hydrogen-bonding solvents it deviates from the line to the extent of the hydrogen-bond acidity α and the hydrogen-bond basicity β of the solvent.[7,8] Figure 3 shows the absorption maximum of DMPT in various solvents as a function of π^*. The results in aprotic solvents show a satisfactorily linear correlation. This is because DMPT is not proton-donating but only proton-accepting, mainly on the carbonyl group.

On the other hand, the results in dioxane–water deviate from the above straight line. Figure 4 shows the relationship of α vs. π^* of dioxane–water. Only α should be considered here because DMPT is only proton-accepting. It is also worth noting that α always increases with $\pi^*$and that this increase is linear in the π^*ranges of 0.59 to 0.75 and of 0.82 to 1.1. For the data points corresponding to band I, the wavenumber

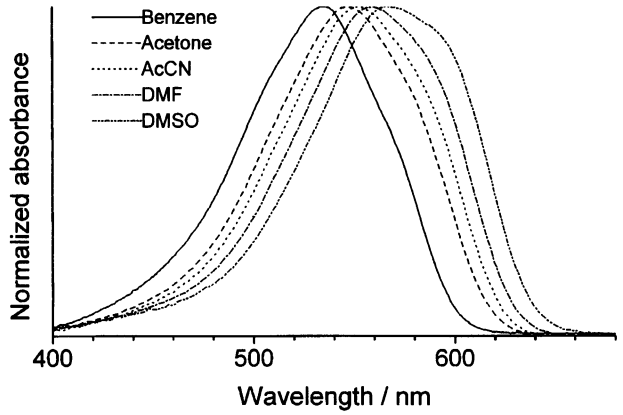

Fig. 1. Absorption spectra for DMPT in aprotic solvents.

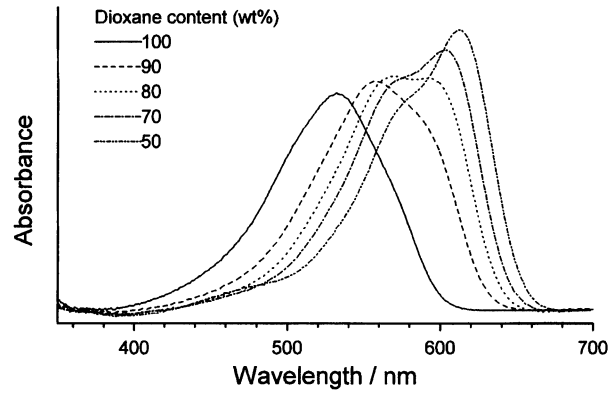

Fig. 2. Absorption spectra for DMPT in dioxane–water.

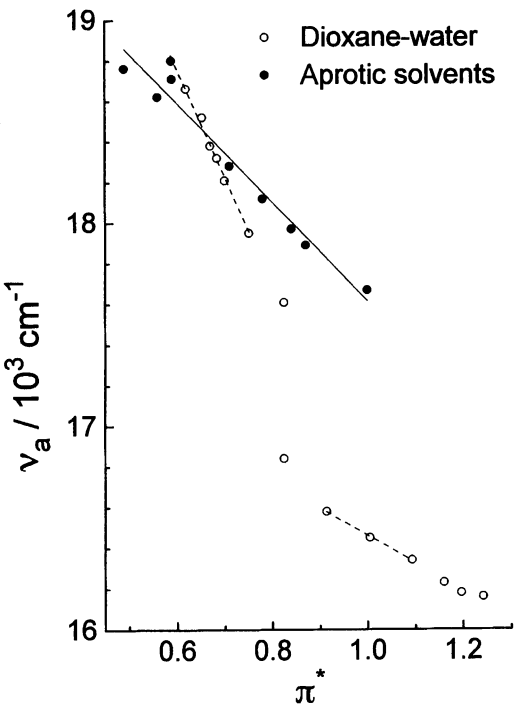

Fig. 3. Absorption maximum in wavenumber for DMPT as a function of π^* in aprotic solvents and dioxane–water. The solid line correlates maxima in aprotic solvents. The dashed lines correlate maxima in dioxane–water in the π^* ranges smaller than 0.75 and of 0.9 to 1.1.

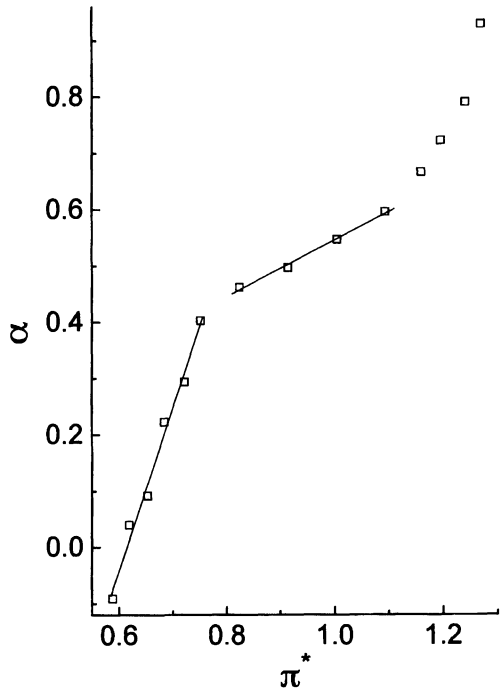

Fig. 4. Relationship of α vs. π^* of dioxane–water. The lines correlate the data in the π^* ranges smaller than 0.75 and of 0.82 to 1.1.

decreases linearly with increasing π^*. The sensitivity to π^* is higher than for the aprotic solvents. Because α increases linearly with π^* in this range, it seems that the same species of DMPT is responsible for the apparent π^*dependence in aprotic solvents and in this range of dioxane–water, and that the hydrogen-bond acidity of water enhances the red shift of the absorption of this species. For the data points corresponding to band II, the plot is seemingly linear. The sensitivity to $\pi^*$is a little smaller than that for the aprotic solvents, indicating that the π^* dependence itself without the effect of α is different from that for the aprotic solvents, that is, the apparent π^* dependence arises from a different species. Therefore it is concluded that the two bands do not represent vibronic states but originate from different species or configurational states.

Considering the π^* dependence of the absorption maximum and the resemblance between the spectra in polar aprotic solvents, e.g. DMSO, and in dioxane-water mixtures, e.g., 80 wt% dioxane, it is suggested that the long-wavelength shoulder appearing in the polar aprotic solvents corresponds to band II appearing in dioxane–water. However, the relative intensity of band II was much lower in an aprotic solvent, e.g. DMSO, than in a mixed solvent possessing a π^* value identical to that of the aprotic solvent, e.g., 60 wt% dioxane. It seems that the chemical species corresponding to band II appears in polar solvents with large π^* values and becomes predominant in the presence of strong protic solvents such as water.

The concentration dependence of the absorption spectrum of DMPT was examined in dioxane–water. A 100-fold increase of the dye concentration caused little change in the relative intensities of bands I and II in 70 wt% dioxane. This reveals that aggregation of DMPT does not occur in this mixed solvent and that the bands do not correspond to species with different aggregation states. In contrast, the spectral shape changes with a 100-fold increase in the dye concentration in 20 wt% dioxane, as shown in Fig. 5. The main band at 620 nm decreases while the shoulder around 570 nm develops and a new broad band appears around 470 nm. This indicates that the species corresponding to band II aggregates in this mixed solvent at a high dye concentration and that it is different in the monomeric form from the species corresponding to band I.

Figure 6 shows the absorption spectra of DMPT in 70 wt% dioxane in the presence and absence of hydrogen chloride (HCl). As the HCl concentration increases, the main band at 602 nm reduces while a new broad band develops in the range of 400—500 nm. The two isosbestic points can be seen at 515 and 630 nm. This indicates that two equilibrated species are responsible for the spectral change along with the HCl concentration. This can be understood in terms of protonation of DMPT mainly on the carbonyl oxygen.

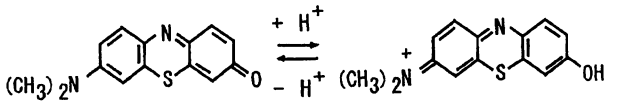

(3)

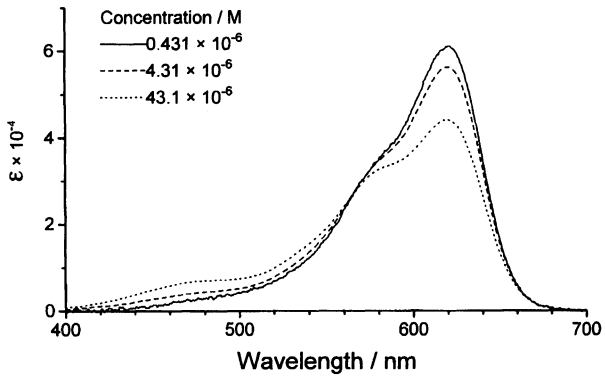

Fig. 5. Absorption spectra for DMPT in 20 wt% dioxane–water at different concentrations of the dye.

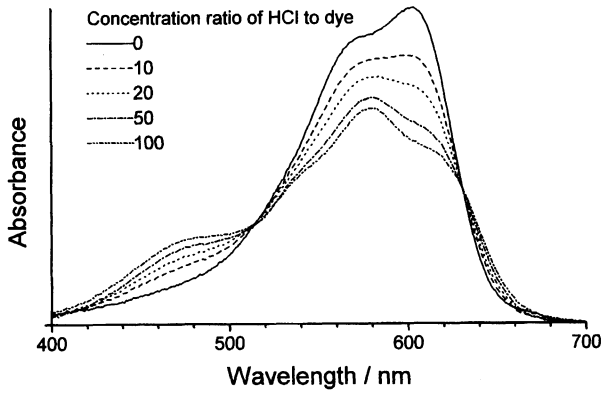

Fig. 6. Absorption spectra for DMPT in 70 wt% dioxane–water at different concentrations of HCl.

It is worthwhile to compare this spectral change with that caused by the addition of water to the dioxane solution. The two changes are quite different, indicating that the species predominant in dioxane–water mixtures with large π^* values is different from the protonated species present in the acidic solutions.

Fluorescence Behaviors. Figure 7 shows corrected fluorescence spectra of DMPT in dioxane–water. The fluorescence spectrum undergoes a significant red shift when increasing the polarity of the solvent. The spectrum is structured with a long-wavelength side band in the mixed solvents with dioxane contents above 95 wt%. This was also observed in other nonpolar solvents such as benzene. The excitation spectrum and fluorescence lifetime of the side band were almost the same as those of the main band. In contrast, the spectrum is broad in the mixed solvents with dioxane contents below 95 wt%. This was also observed for other polar solvents such as DMSO.

Figure 8 shows the maximum of the main fluorescence band of DMPT in various solvents as a function of π^*. The long-wavelength side bands appearing in nonpolar solvents are not shown here for simplicity. The results in the aprotic solvents give a satisfactorily straight line. On the other hand, a plot of the results in dioxane–water deviates from the above straight line. The plot is linear in the π^* range smaller than 0.75. The sensitivity to π^* is higher than for the aprotic solvents. Because α increases linearly with π^* in this range, it seems that the same emitting state of DMPT is responsible for the observed fluorescence in aprotic solvents and in this range of dioxane–water, and that the hydrogen-bond acidity of water enhances the red shift. In the π^* range larger than 0.82, the plot is seemingly linear. The sensitivity to π^* is smaller than that for the aprotic solvents, suggesting that the π^* dependence itself without the effect of α is different, that is, this π^* dependence arises from a different emitting state.

Figure 9 shows the fluorescence quantum yield of DMPT in various solvents as a function of π^*. On the whole, the quantum yield tends to increase with π^* in the aprotic solvents. However, when increasing the π^* value, the quantum yield initially increases but decreases above a π^* value around 0.67 in dioxane–water.

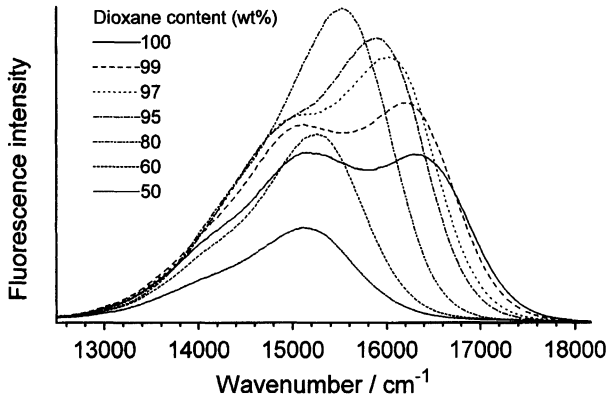

Fig. 7. Corrected fluorescence spectra for DMPT in dioxane–water.

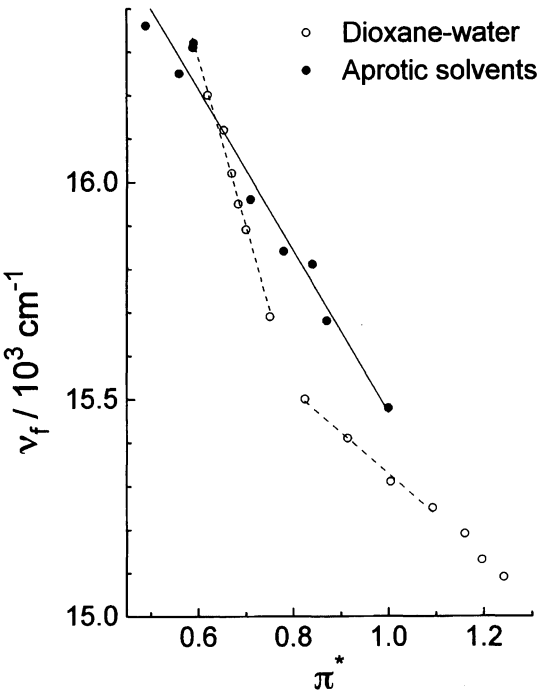

Fig. 8. Maxima of the main fluorescence band in wavenumber for DMPT as a function of π^* in aprotic solvents and dioxane–water. The solid line correlates maxima in aprotic solvents. The dashed lines correlate maxima in dioxane–water in the π^* ranges smaller than 0.75 and of 0.82 to 1.1.

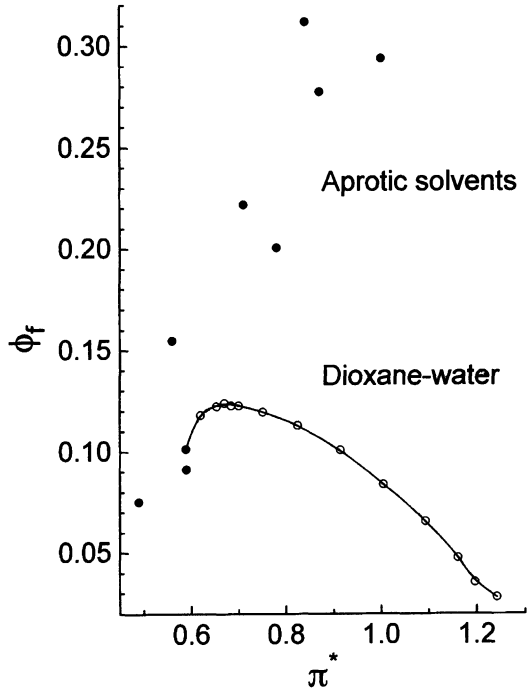

Fig. 9. Fluorescence quantum yield for DMPT as a function of π^* in aprotic solvents and dioxane–water.

The fluorescence decay for DMPT was measured in various solvents. The decay curves were well analyzed by single exponential kinetics with chi-square values ranging from

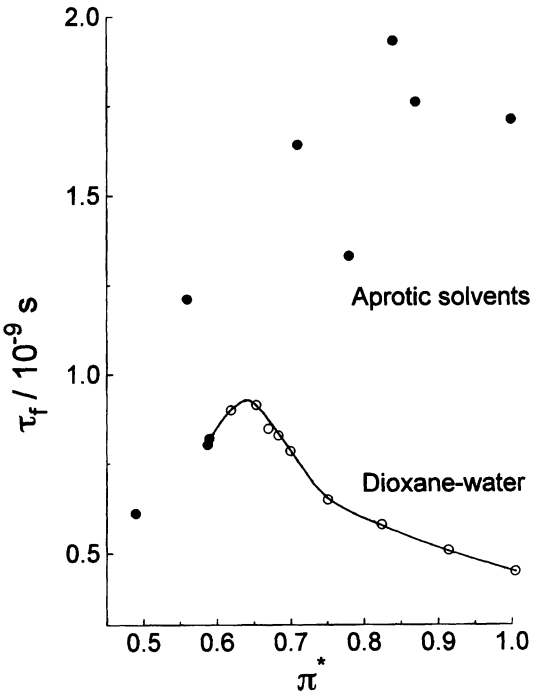

Fig. 10. Fluorescence lifetime for DMPT as a function of π^* in aprotic solvents and dioxane–water.

0.90 to 1.55. Figure 10 shows the fluorescence lifetime as a function of π^*. The dependence on π^* is seemingly similar to that for the fluorescence quantum yield.

Changes in the fluorescence quantum yield and lifetime can in principle be the result of changes in either the radiative (k_r) or nonradiative rate constants (k_{nr}). These values are readily calculated using the following relations.

$$k_r = \phi_f/\tau_f \text{ and } k_{nr} = (1-\phi_f)/\tau_f. \quad (4)$$

Since the fluorescence quantum yield and lifetime include contributions of all emitting states, k_r and k_{nr} here are apparent values.

Figure 11 shows k_r and k_{nr} of DMPT in various solvents as a function of π^*. Since the solvatochromic scales of Taft and Kamlet are also applicable to the rate constants of a number of reactions,[7,8] the π^* dependence of k_r and k_{nr} may provide information about properties of the emitting state. In aprotic solvents, the correlation between k_r and π^* is good, whereas the results for k_{nr} are fairly dispersed. In dioxane–water, the dependence of k_r on π^* is linear in the π^* range of 0.65 to 0.75. The results deviate from the straight line below and above this range. A similar dependence on π^* is seen for k_{nr}. Because α increases linearly with π^* in the π^* range of 0.59 to 0.75 in dioxane–water, these results suggest that there are two different emitting states in this π^* range, where the π^* dependence of the fluorescence maximum exhibited only a single type of behavior (Fig. 8).

The red shifts of the absorption and fluorescence spectra may be used for determination of the increase in the dipole moment upon excitation. According to the theory of Lippert[11] and Mataga et al.,[12] the Stokes shift $\Delta\nu=(\nu_e-\nu_g)$

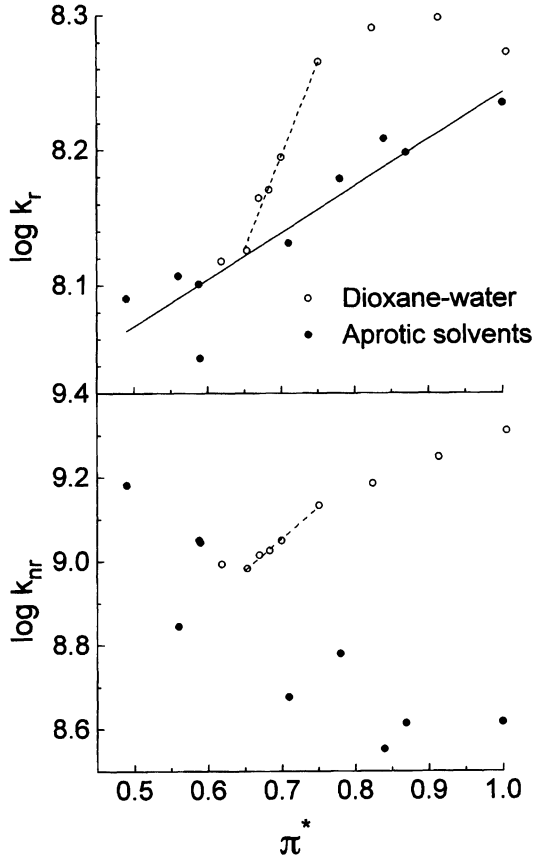

Fig. 11. k_r and k_{nr} for DMPT as a function of π^* in aprotic solvents and dioxane–water. The solid line correlates k_r in aprotic solvents. The dashed lines correlate the rate constants in dioxane–water in the π^* range of 0.65 to 0.75.

in wavenumber should be linearly correlated with a solvent parameter Δf defined as

$$\Delta f = \frac{\varepsilon-1}{2\varepsilon+1} - \frac{n^2-1}{2n^2+1}. \quad (5)$$

The slope of the straight line is given by

$$s = \frac{2(\mu_e-\mu_g)^2}{hca^3}, \quad (6)$$

where μ_g and μ_e are ground- and excited-state dipole moments, respectively, and a is the Onsager radius.

The π^* dependence of k_r and k_{nr} suggested the presence of two emitting states in dioxane–water with small π^* values, one dominant at π^* values below 0.65 and the other dominant at π^* values above 0.65. Figure 12 shows $\Delta\nu$ vs. Δf for DMPT in aprotic solvents. The data points are significantly scattered. This is presumably because the two emitting states also exist in aprotic solvents. Removing the data points with very small π^* values may enable determination of excited-state properties for a single emitting state. Although this results in a rather poor correlation as shown in Fig. 12, it is still possible to determine the difference $\mu_e-\mu_g$. The slope of the regression line, the correlation coefficient, and the calculated value of the difference are 1460 cm^{-1}, 0.77, and 3.0 D, respectively. In this calculation, the radius a is

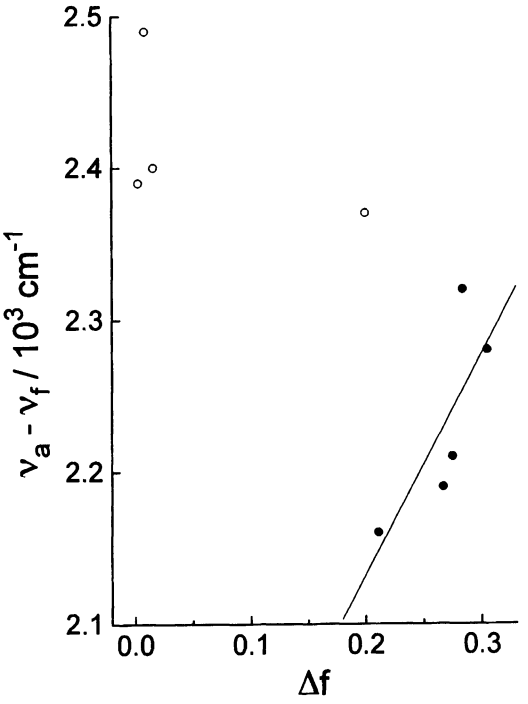

Fig. 12. Stokes shift $\Delta\nu=(\nu_e-\nu_g)$ for DMPT as a function of Δf in aprotic solvents. The open symbols correspond solvents with small π^* values and the closed symbols solvents with large π^* values. The straight line correlates $\Delta\nu$ with Δf for results in the latter solvents.

estimated to be about 4 Å. The reasonable value thus obtained strongly suggests the two emitting states in aprotic solvents.

Figure 13 shows the excitation spectra in dioxane–water. When decreasing the dioxane content, the main band appearing in dioxane-rich mixtures shifts to a longer wavelength, and a shoulder appears at the long-wavelength side and develops in water-rich mixtures. The former band apparently corresponds to band I observed in the absorption spectrum. Although the latter band can not be seen in the figure, it indeed exists above the sensitivity limit of the spectrometer

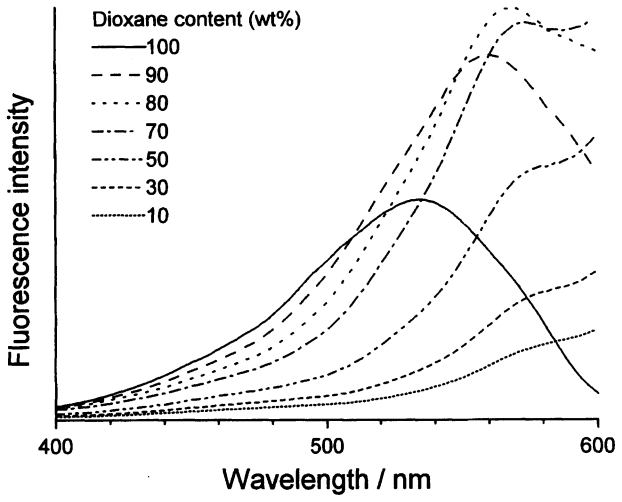

Fig. 13. Corrected excitation spectra for DMPT in dioxane–water. Emission wavelength, 655 nm.

of 600 nm and corresponds to band II. This clearly shows that the two species corresponding to the bands are both fluorescent.

Discussion

The appearance of the two distinct bands in the absorption spectrum and the large difference in π^* dependence between the two bands confirm the existence of two different species in the ground state. However, it was shown that these two species do not correspond to aggregated molecules or protonated species of DMPT. It has been described that hydrogen bonding complexes are formed between dye and solvent molecules in the ground state for 4-dimethylaminobenzonitrile[13,14] and coumarine dyes.[15] For these compounds, red shifts of the absorption and fluorescence spectra were observed on addition of strong protic solvents such as water and alcohols to solutions in aprotic solvents. However, the two bands in the absorption spectrum of DMPT can not be ascribed to complex formation between the dye and solvent molecules because the appearance of band II started after the addition of a fair amount of water to the dioxane solutions and because band II also appeared in several aprotic solvents. Presumably the two ground-state species come from conformational changes involving rotational isomerization around the amine-aromatic ring. Therefore, it is expected that the species dominant in aprotic solvents or dioxane–water mixtures with small π^* values is a nontwisted conformer (S_{NT}) and that the species dominant in dioxane-water mixtures with large π^* values is a twisted conformer (S_T).

However, the conformation changes which are considered as an origin of the two ground-state species for DMPT seem energetically unfavorable by themselves in the ground state. Photoelectron spectroscopy has shown that the dialkylamino group is fairly twisted in relation to the benzene ring for 4-diethylaminobenzonitrile and a little twisted even for 4-dimethylaminobenzonitrile and that the angular distribution function for these compounds is very broad which allows the twisted conformation population.[16] These facts may support the existence of stable twisted conformations also for DMPT. In addition, it has been proposed that for 4-substituted *N*, *N*-dialkylanilines, an observed red shift of the absorption spectrum is due to formation of complexes between dye and water molecules and that this complexation stabilizes a conformation with the dialkylamino group twisted in relation to the benzene ring in the ground state.[14] It is expected that the twist of the dimethylamino group of DMPT is also promoted by some interactions between dye and solvent molecules such as hydrogen bonding. This idea is supported by the fact that band II appearing in polar aprotic solvents was much weaker compared to that appearing in polar dioxane–water mixtures.

The π^* dependence of the fluorescence maximum suggested the existence of two different emitting states, one dominant in aprotic solvents and dioxane–water mixtures with small π^* values and the other dominant in dioxane–water mixtures with large π^* values. As described above, there are two different conformers in the ground state. Moreover, both are fluorescent as judged from the excitation spectra.

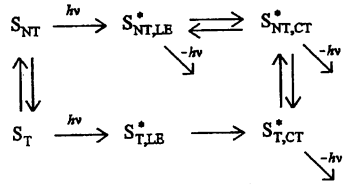

Chart 1.

These facts suggest that the two ground-state conformers give rise to the two emitting states. In addition, the π^* dependence of k_r and k_{nr} and the Lippert–Mataga plot of the spectral shifts suggest the existance of another emitting state in solvents with small π^*values. Because the S_T species is considered negligible in such solvents, this emitting state is probably produced from the S_{NT} species. It has been reported that the two types of emission different in polarity dependence come from the locally excited (LE) and the charge transfer (CT) states for (phenylamino)naphthalenesulfonates.[17] The major decay from the LE state is radiative in nonpolar solvents although the rate of the electron transfer reaction which converts the LE state to the CT state becomes greater than the radiative rate in more polar solvents.[18] These fluorescent states may also contribute to the fluorescence for DMPT. A conceivable mechanism of transition and relaxation is depicted in Chart 1.

In this Chart 1, fast equilibria are assumed between the emitting states. The fluorescence spectrum exhibited only one band in polar aprotic solvents and dioxane-water mixtures with middling to large π^* values. In addition, although the spectrum had a long-wavelength side band in nonpolar aprotic solvents and dioxane–water mixtures with small π^* values, the excitation spectrum and fluorescence lifetime of the side band were almost the same as those of the main band. These phenomena are probably the result of the fast equilibria.

According to the proposed scheme, the emission from the $S^*_{T,CT}$ state was observed for DMPT. Based on the dependence of the photophysical properties on the solvent polarity, a model of nonradiative decay has been proposed which employs a planar highly emissive intramolecular charge transfer (ICT) excited state capable of decay to a nonfluorescent twisted ICT (TICT) state.[19] The ICT-TICT model has been applied to a variety of compounds.[20] In most cases, the TICT state was found to be nonfluorescent. However, for a few compounds including 6-aminocoumarin,[21] observed emission has been ascribed to the TICT states. From a theoretical view point, emission from a perpendicularly twisted ICT conformation is forbidden by symmetry. However, by coupling to suitable vibrations, this transition can borrow intensity from higher-excited allowed states.[20] The quantum yield of fluorescence from the TICT state ($S^*_{T,CT}$) of DMPT was 0.03 in 20 wt% dioxane to 0.08 in 60 wt% dioxane. This appreciable value should also be accounted for by the vibronic coupling mechanism.

Conclusions

The work presented here indicates that the wavelengths of maximal absorption and fluorescence of DMPT decrease when the dye is dissolved in a more polar solvent. It is this property which makes DMPT useful as an optical probe of the microenvironments of various media. In addition, DMPT absorbs at 532—619 nm and emits at 611—663 nm in solvents used in this study, which are much longer wavelengths relative to those for an analogous dye, 7-dimethylamino-3*H*-phenoxazin-3-one, which absorbs at 513—595 nm and emits at 580—637 nm in the same solvents.[22] This is ascribed to the presence of a sulfur atom in the aromatic ring of DMPT instead of an oxgen atom. The long wavelengths of the absorption and fluorescence will remove problems of signal distortion caused by fluorescence of target molecules or other probes. The large Stokes shifts (1070—2490 cm^{-1}) will minimize background signals and allow detection with high sensitivity. The fluorescence quantum yields (0.03—0.31) are enough to use low concentrations of dye if needed.

References

1) W. O. McClure and G. M. Edelman, *Biochemistry*, **5**, 1908 (1966).
2) D. C. Turner and L. Brand, *Biochemistry*, **7**, 3381 (1968).
3) G. Weber and F. J. Farris, *Biochemistry*, **18**, 3075 (1979).
4) D. L. Sackett and J. Wolff, *Anal. Biochem.*, **167**, 228 (1987).
5) T. A. Brugel and B. W. Williams, *J. Fluoresc.*, **3**, 69 (1993).
6) M. R. Mclean, M. Bader, L. R. Dalton, R. L. S. Devine, and W. H. Steier, *J. Phys. Chem.*, **94**, 4386 (1990).
7) R. W. Taft and M. J. Kamlet, *J. Am. Chem. Soc.*, **98**, 2886 (1976).
8) M. H. Abraham, P. L. Grellier, J.-L. M. Abboud, R. M. Doherty, and R. W. Taft, *Can. J. Chem.*, **66**, 2673 (1988).
9) M. H. Abraham, G. J. Buist, P. L. Grellier, R. A. McGill, D. V. Prior, S. Oliver, E. Turner, J. J. Morris, P. J. Taylor, P. Nicolet, P.-C. Maria, J.-F. Gal, J.-L. M. Abboud, R. M. Doherty, M. J. Kamlet, W. J. Shuely, and R. W. Taft, *J. Phys. Org. Chem.*, **2**, 540 (1989).
10) Ch. Reichardt and K. Dimroth, *Fortschr. Chem. Forsch.*, **11**, 1 (1968).
11) E. Lippert, *Z. Naturforsch. A*, **10**, 541 (1955).
12) N. Mataga, Y. Kaifu, and M. Koizumi, *Bull. Chem. Soc. Jpn.*, **29**, 465 (1956).
13) Y. Wang and K. B. Eisenthal, *J. Chem. Phys.*, **77**, 6076 (1982).
14) C. Cazeau-Dubroca, S. Ait Lyazidi, P. Cambou, A. Peirigua, Ph. Cazeau, and M. Pesquer, *J. Phys. Chem.*, **93**, 2347 (1989).
15) M. S. A. Abdel-Mottaleb, M. S. Antonious, M. M. Abo-Aly, L. F. M. Ismaiel, B. A. El-Sayed, and A. M. K. Sherief, *J. Photochem. Photobiol. A*, **50**, 259 (1989).
16) W. Rettig and R. Gleiter, *J. Phys. Chem.*, **89**, 4676 (1985).
17) E. M. Kosower, *Acc. Chem. Res.*, **15**, 259 (1982).
18) E. M. Kosower, H. Dodiuk, K. Tanizawa, M. Ottolenghi, and N. Orbach, *J. Am. Chem. Soc.*, **97**, 2167 (1975).
19) G. Jones, II, W. R. Jackson, C.-Y. Choi, and W. R. Bergmark, *J. Phys. Chem.*, **89**, 294 (1985).
20) W. Rettig, *Angew. Chem., Int. Ed. Engl.*, **25**, 971 (1986).
21) W. Rettig and A. Klock, *Can. J. Chem.*, **63**, 1649 (1985).
22) S. Otsuki and T. Taguchi, unpublished data.